Evolution of the martian mantle and crust. A crystal chemical perspective from olivine in basaltic shergottites. C.K. Shearer[1] , P.V. Burger[1] , J.J. Papike[1], L.E. Borg[2], A.J. Irving[3] , and C.D.K. Herd[4], [1]Institute of Meteoritics, Department of Earth and Planetary Sciences, University of New Mexico, Albuquerque, New Mexico 87131 (cshearer@unm.edu), [2] Lawrence Livermore National Laboratory, Livermore, CA 94551. [3]Department of Earth and Space Sciences, University of Washington, Seattle, WA 98195, [4]Department of Earth and Atmospheric Sciences, University of Alberta, Edmonton, Alberta, Canada T6G 2E3.

Introduction: The shergottites (basaltic and lherzolitic martian meteorites) exhibit a range of major and trace element compositions, crystallization ages, and initial Sr, Nd, Hf, and Pb isotopic compositions [1,2]. Associated with these variations in geochemical parameters are potential variations in f_{O2} conditions under which the shergottites crystallized (2 to 4 log units) [3,4,5,6,7]. These correlations have been interpreted as indicating the presence of reduced, incompatible element-depleted and oxidized, incompatible element-enriched reservoirs that were produced during early stages of martian differentiation (≈4.5Ga) [1,2,3,4,5,6,7]. Martian basaltic magmatism represented by the shergottites is thought to represent mixing between these two reservoirs. Whether this mixing process is a product of varying degrees of assimilation of martian crust by mantle derived magmas [1,2,3,4,5,6,7] or mixing of distinctly different mantle reservoirs during melting is still a point of debate.

The goal of this study is to constrain the physical mechanisms by which shergottites obtain their compositional characteristics. This is accomplished through a major and trace element study of one of the earliest crystallizing phases (olivine) in some of the more primitive shergottites. Here, we define the petrogenesis of olivine in the olivine-phyric shergottites, evaluate its use in recording the earliest stages of martian basalt crystallization, and compare olivine major and trace element characteristics among the shergottites.

Analytical Approach: Olivine-bearing shergottites (Y 980459 (Y98), NWA 2626, NWA 2046, NWA 1195, NWA 1110, Dhofar 019, SaU 005, EETA 79001A, DaG 476) were analyzed in this study. All of these martian meteorites have been studied to varying degrees [i.e. 4,8,9,10,11,12,13,14]. Olivine in these basalts was first imaged and mapped by SEM followed by major element analysis using a JEOL JXA-8200 electron microprobe. A suite of trace elements was analyzed (Sc, V, Cr, Ti, Mn, Co, Ni, and Y) using a Cameca 4f ims ion microprobe and previously documented analytical approaches [13, 15]. Where possible, inclusions or embayments of "melt" in olivine were analyzed for a subset of REE. The intent of these analyses was not to determine rigorously the melt compositions trapped by the olivine, but to simply compare differences in "trapped melts". All instruments used in these analyses are housed in the Institute of Meteoritics at UNM.

Results:

Characteristics of olivine. In the shergottites, olivine has a wide range of morphologies and textural relationships with adjacent mineral phases. The large olivine "megacrysts" commonly occur in clusters and range in morphology from euhedral (i.e. Y98) to corroded/resorbed with thin Fe-rich rims (i.e. NWA 1110). Based on textural relationships, "spinel" and pyroxene may co-precipitate with olivine during at least a portion of its crystallization history.

Olivine major element chemistry. The Mg# of early olivine in the shergottites ranges from 85 to 50 (Fig. 1). The olivine cores of Y98 and NWA 2046 have the highest Mg#. Based on Fe-Mg exchange K_D between olivine-basalt and experimental studies [16, 17] most of the olivines are not in equilibrium with the bulk rock compositions with the exception of Y98 (Fig. 1). Comparisons of olivine in Y98 to olivine in other shergottites provide insights into the petrogenesis of the olivine megacrysts. There are significant differences in the Mg-zoning profiles between Y98 and olivine in other shegottites. Y98 has only slight enrichements of Fe in the rims whereas most other shergottites exhibit substantial Fe-enrichments. MnO increases with decreasing Mg# from core to rim. There can be substantial overlap in Mg# - MnO in different shergottites. This suggests that these different basalts represent melts with similar characteristics. CaO exhibits substantial differences among the shergottites (Figure 2). In Y98, CaO increases slightly with decreasing Mg#. NWA 2626 and EETA 79001 exhibit a near constant CaO with decreasing Mg#. NWA 1110 exhibits the most complex zoning with CaO increasing with decreasing Mg# followed by a substantial decrease in both CaO and Mg#.

Olivine trace element chemistry. Ni – Co behave similarly in all martian olivines analyzed with decreasing Ni and increasing Co from core to rim (Fig. 3). The olivine cores of Y98 have the highest Ni abundance. Using core compositions of Y98 and bulk Y98 compositions appropriate D for Ni and Co for these basalts are 7.3-5.5 and 2.4-1.8, respectively. Surprisingly, most of the Ni-Co zoning trajectories for the olivine overlap except for NWA 1110. NWA 1110 appears to

be less depleted in incompatible elements than most of the other olivine-phyric shergottites [i.e.1, 2, 3, 4] and cores have high Y. Our initial analyses of inclusions in the olivine indicate that the REE pattern in NWA 1110 generally tends to be flat, whereas in Y98 the REE pattern is LREE depleted. The pattern for inclusions in NWA 1110 is similar to that observed by [17].

The multi-valence partitioning behavior of V in olivine reflects the early f_{O2} crystallization conditions of basaltic magmas [18]. Vanadium in Y98 (Fig. 4), lunar basalts, and terrestrial basalts (Fig. 4B) increases with decreasing Ni from core to rim Using the behavior of V in olivine Y98, [18] estimated that the conditions of initial crystallization was at an f_{O2} of IW+0.9. This is similar to f_{O2} estimates made by [19] for QUE using V and Cr partitioning between melt and early pyroxene, Compared to Y98, vanadium in olivine from all the other martian basalts decreases with decreasing Ni from core to rim. This may be interpreted as either indicating that the olivine in these samples is not in equilibrium with the adjacent melt or that pyroxene ± spinel is influencing the behavior of V.

Discussion:

Nature of olivine in the olivine shergottites. There has been significant discussion concerning the origin of the olivine in the olivine-bearing shergottites (phenocrysts, megacrysts, xenocrysts). Based on such characteristics as the Mg# , V zoning, calculated $D_{Ni,Co}$, the olivine in Y98 are phenocrysts. Many of these same characteristics indicate that the olivines in other shergottites are not in equilibrium with the adjacent melt. However, in most cases they are not xenocrystic, but additions of olivine from the same basaltic system. This is consistent with the overlap of trace elements (Figs. 2, 3 & 4) and isotopic data [i.e. 6]. NWA 1110 may be an exception [19]. Trace elements such as V and CaO in olivine appear to record the appearance of spinel and pyroxene on the liquidus.

Petrogenetic relationships among the olivine-bearing shergottites. Many of the olivine shergottites represent basalts produced by melting of reduced (IW to IW + 1) depleted mantle sources [17]. Olivine data indicate that many of the primary melts derived from this source had similar Ni, Co, and Mn. They exhibited more deviation in Cr and V. More evolved martian basalts such as QUE 94201 were probably derived from the fractional crystallization of these basaltic melts. Other olivine-phyric shergottites (i.e. NWA 1110) that appear to be derived from more enriched sources [1,2,3,5] have distinctly different olivine. These olivines are more enriched in Co, enriched in incompatible elements such as Y, and crystallized from basalt which have flat REE patterns and are more oxidizing than IW+1.

Conclusions:

The olivine in shergottites generally tends to reflect the overall character of the basalt in which they occur (enriched/depleted, f_{O2}). In the case of NWA 1110, this implies that the enriched component was added to system prior to olivine crystallization. In addition, this observation implies that in most cases the olivine was not randomly incorporated into the basalt, but is cogenetic in some manner.

The V data also indicates a limited range of f_{O2} of crystallization for the "depleted" olivine-bearing shergotittes (~IW+1).

The significant overlap in olivine compositions in many of the "depleted" olivine-bearing shergottites may be interpreted as indicating that they crystallized from basalts with many similar characteristics**.**

The deviations from Y98 that were observed in olivine from the other shergotttites reflect the response to other co-precipitating phases and late-stage reequilibration with evolving basalt.

Melts from which the olivine-phyric shergottites were derived are parental to both "depleted" and "enriched" shergottites.

References: [1] Herd et al. (2002) *GCA* 66, 2025-2036. [2] Herd, C (2003) *MAPS* 38, 1993-1805. [3] Wadhwa, M. [2001] *Science*, 292, 1527-1530. [4] Goodrich et al. [2003] *MAPS* 38, 1773-1792. [5] Shih et al. (1993) *GCA* 46, 2323-2344. [6] Borg et al. (1997) *GCA* 61, 4915-4931. [7] Jones et al. (1997) *7th Goldschmidt Conf. LPI Contribution* 921, 108. [8] Barrat et al. (2002) *GCA* 66, 3505-3518. [9] Irving et al. (2002) *MAPS* 37, A69. [10] Goodrich et al. (2002) LPSCXXXIV, #1266. [11] Irving et al. (2004) LPSC XXXV, #1444. [12] McSween et al. (1979) Science 204, 1201-1203. [13] Treiman, A.H. (1990) Proc. 20th *LPSC*, 273-280. [14] Irving et al. (2005) LPS XXXVI, #1229 [15] Shearer, C.K. and Papike, J. (2005) *GCA* 69, 3445-3461. [16] McKay et al. (2004) *LPSC XXXV*, abstract # 875. [17] Wadhwa, M. and Crozaz, G. (2002) MAPS 37, A145. [18] Shearer et al. (2006) Amer. Min. 91, 1657-1664. [19] Karner et al. (2007) Amer. Min. 92 (in press). [20] Herd, C (2006) Amer. Min. 91, 1616-1627.

Figure 1.BSE images of olivine in 4 shergottites that illustrate morphology and zoning.

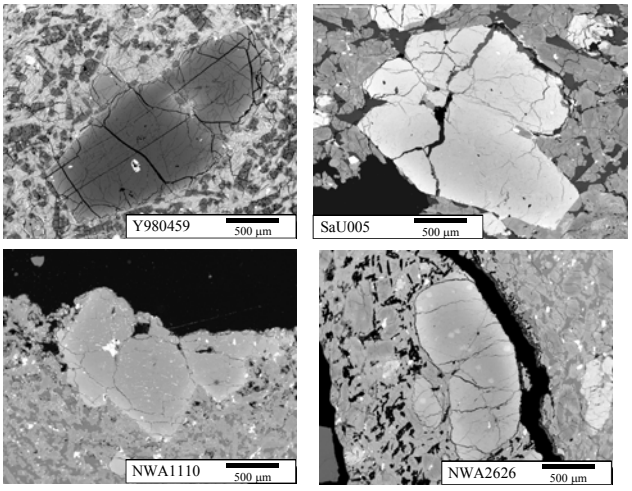

Figure 2. Mg# in olivine versus Mg# of bulk rock. Superimposed field in red represents composition of Mg# of basaltic melt is in equilibrium with olivine. Apollo 12 olivine basalts and Makaopuhi lava lake are shown for comparisons.

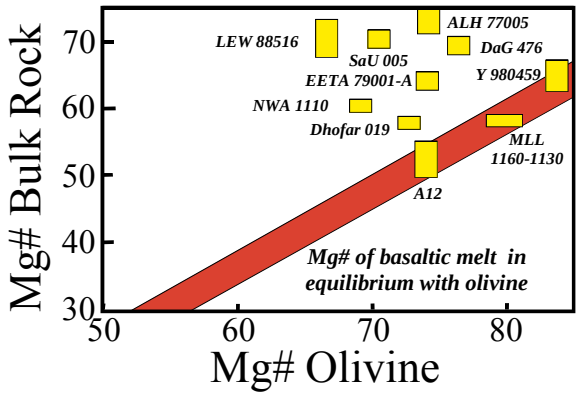

Figure 3. CaO versus Mg# for olivine from shergottites Y98, NWA 2626, EETA 79001, and NWA 1110.

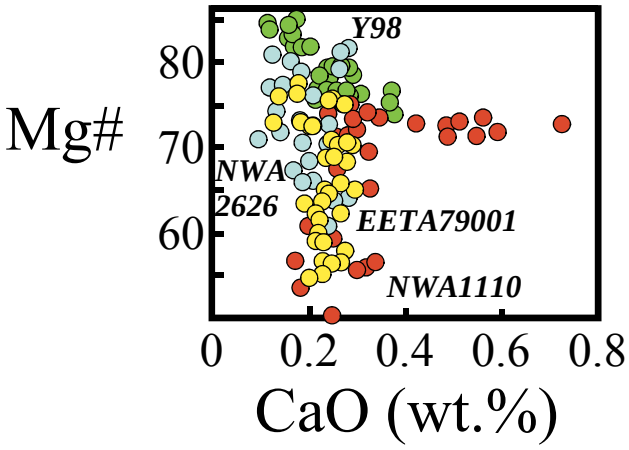

Figure 4. Co versus Ni for the olivine in basaltic shergottites.

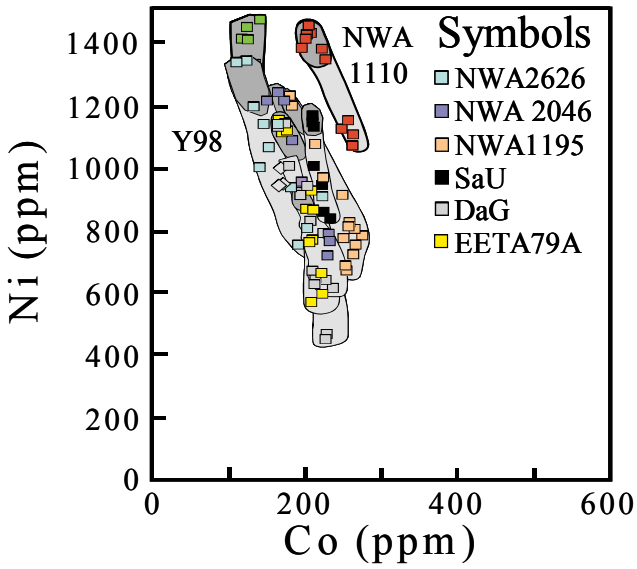

Figure 5. V versus Ni for olivine in basaltic shergottites. Symbols the same as in Figure 4.